

Supporting Information

**High-Mobility In and Ga co-doped ZnO Nanowires for High-Performance
Transistors and Ultraviolet Photodetectors**

Fangzhou Li, You Meng, Xiaolin Kang, SenPo Yip, Xiuming Bu, Heng Zhang, Johnny

C. Ho*

¹ Department of Materials Science and Engineering, ² State Key Laboratory of Terahertz and Millimeter Waves, and ³ Centre for Functional Photonics, City University of Hong Kong, Kowloon 999077, Hong Kong SAR

⁴ Shenzhen Research Institute, City University of Hong Kong, Shenzhen 518057, P.R. China

* Corresponding Email: johnnyho@cityu.edu.hk

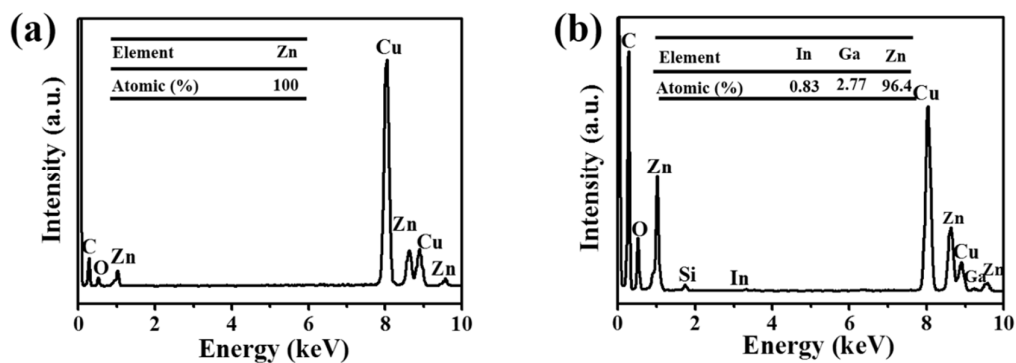


Figure S1 EDS spectra and the corresponding metallic composition of the obtained NWs after the (a) first growth run and (b) second growth run using the same precursor source.

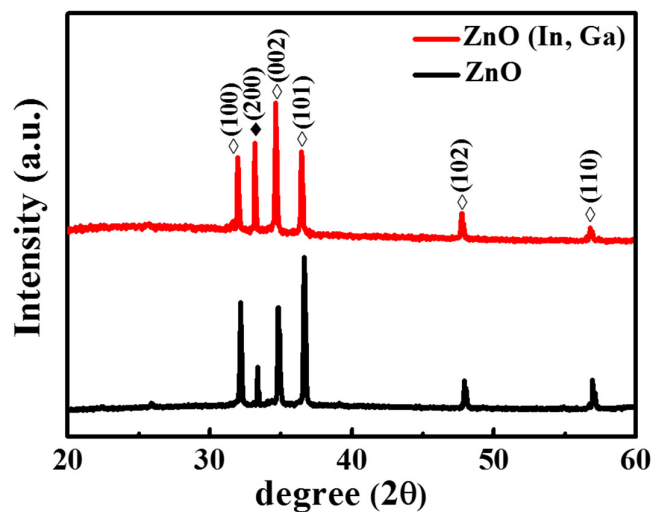


Figure S2 XRD spectra of the NW samples: \diamond : ZnO ; \blacklozenge : Si substrate.

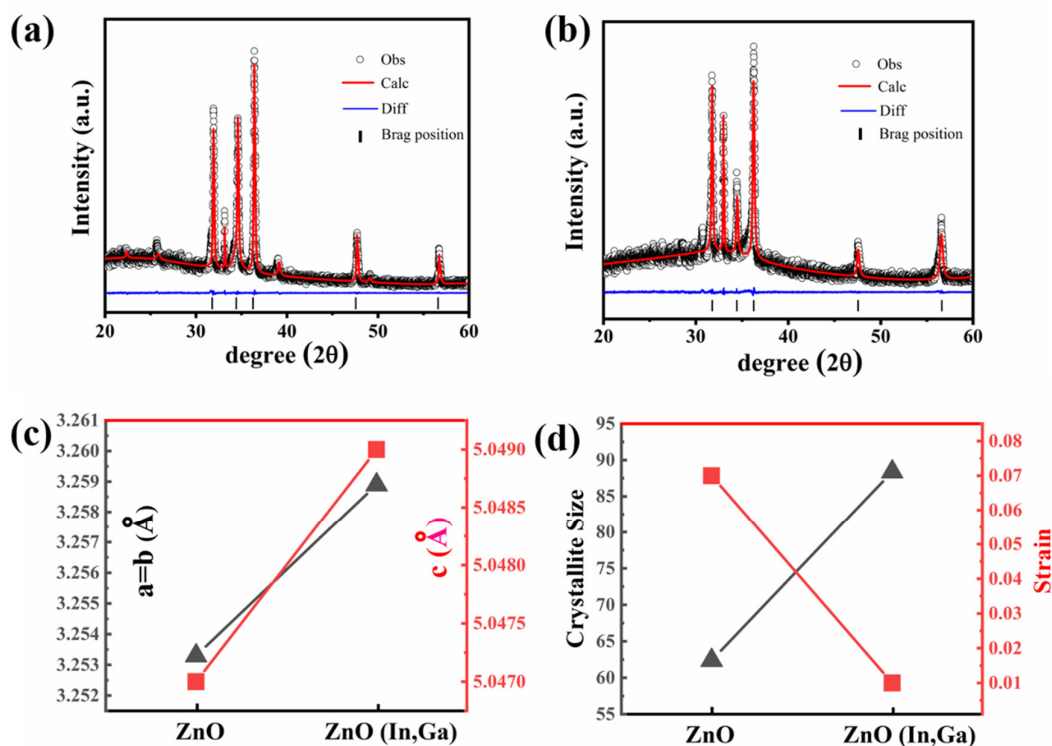


Figure S3 (a) XRD Rietveld refined pattern for In and Ga co-doped ZnO NWs. (b) XRD Rietveld refined pattern for pristine ZnO NWs. (c) Lattice constants and (d) crystallite size and strain for In and Ga co-doped ZnO and pristine ZnO NWs.

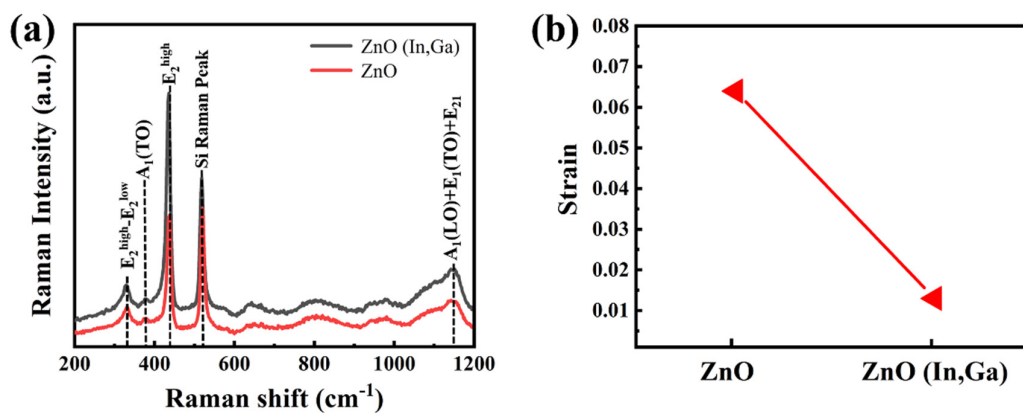


Figure S4 (a) Raman spectra of In and Ga co-doped ZnO and pristine ZnO NWs. (b) Strain estimated from the corresponding $A_1(\text{TO})$ Raman mode presented in the panel a.

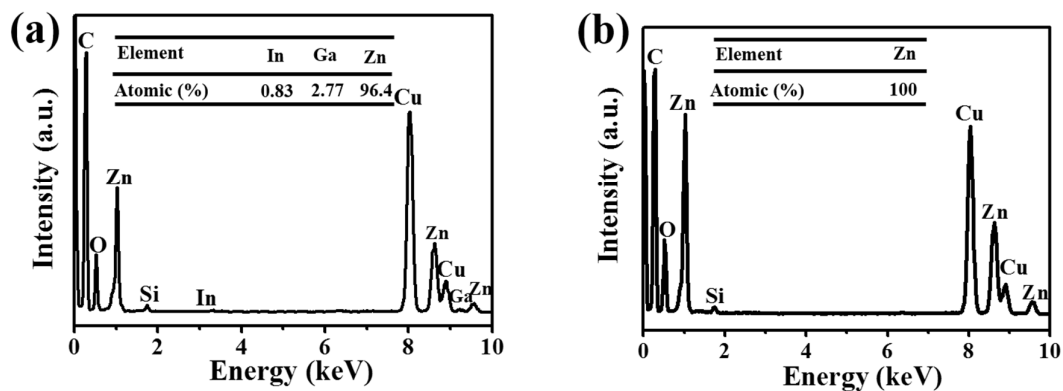


Figure S5 EDS spectra and the corresponding metallic composition of (a) In and Ga co-doped ZnO NWs and (b) pristine ZnO NWs.

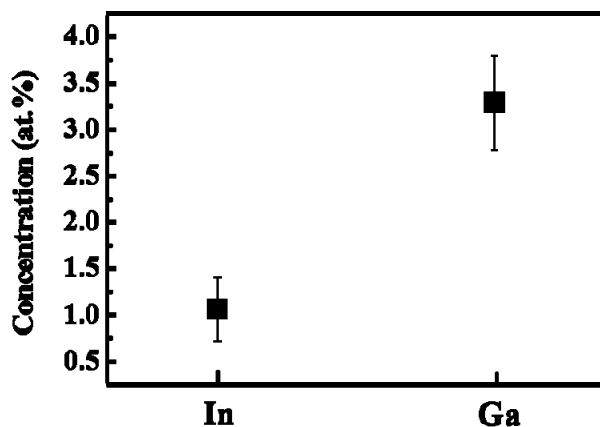


Figure S6 The concentration variation of In and Ga in the co-doped ZnO NWs based on the data extracted from more than 20 NW samples.

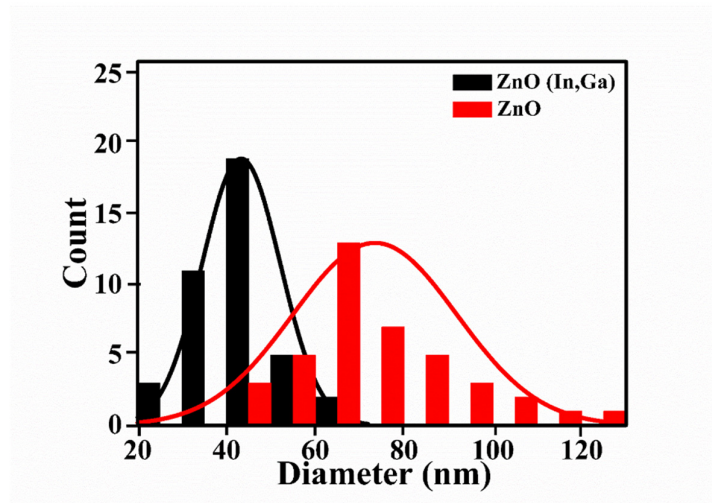


Figure S7 Histogram for the diameter distribution with Gaussian fitting performed.

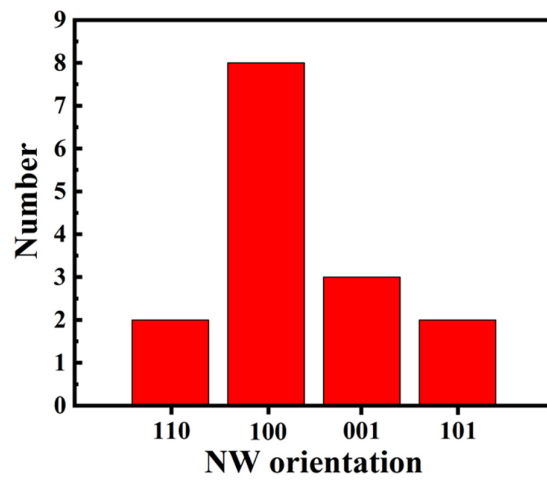


Figure S8 Growth orientation statistics for In, Ga co-doped ZnO NWs.

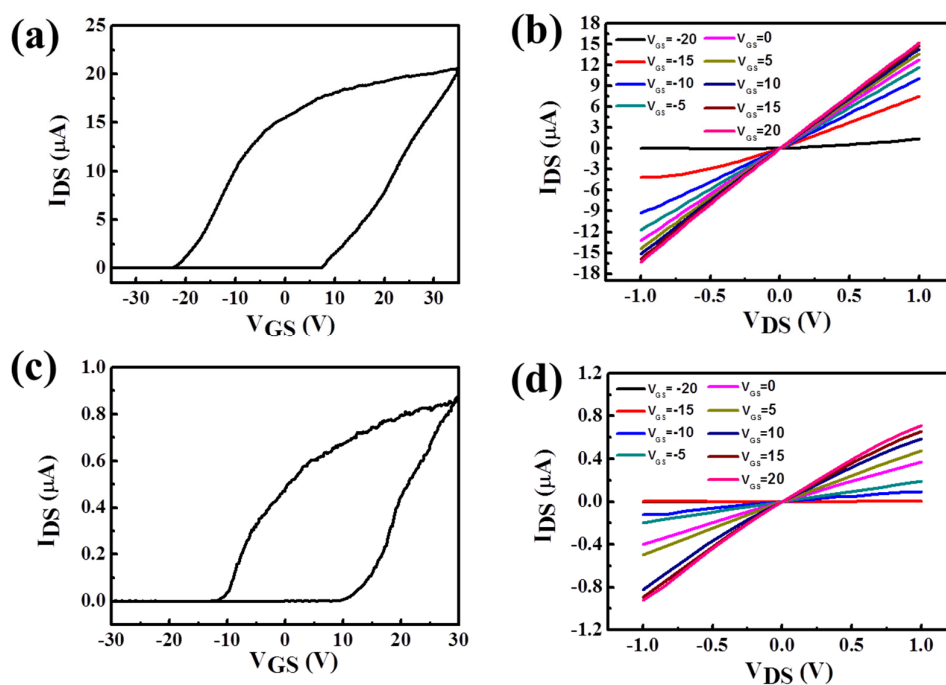


Figure S9 Electrical characterization of single NW based FETs measured in ambient condition. (a) Transfer and (b) output characteristics of the In and Ga co-doped ZnO NW device. (c) Transfer and (d) output characteristics of the pristine ZnO NW device. All the source-drain bias voltage (V_{DS}) is fixed at 1 V. The scan rate is 500 mV s^{-1} .

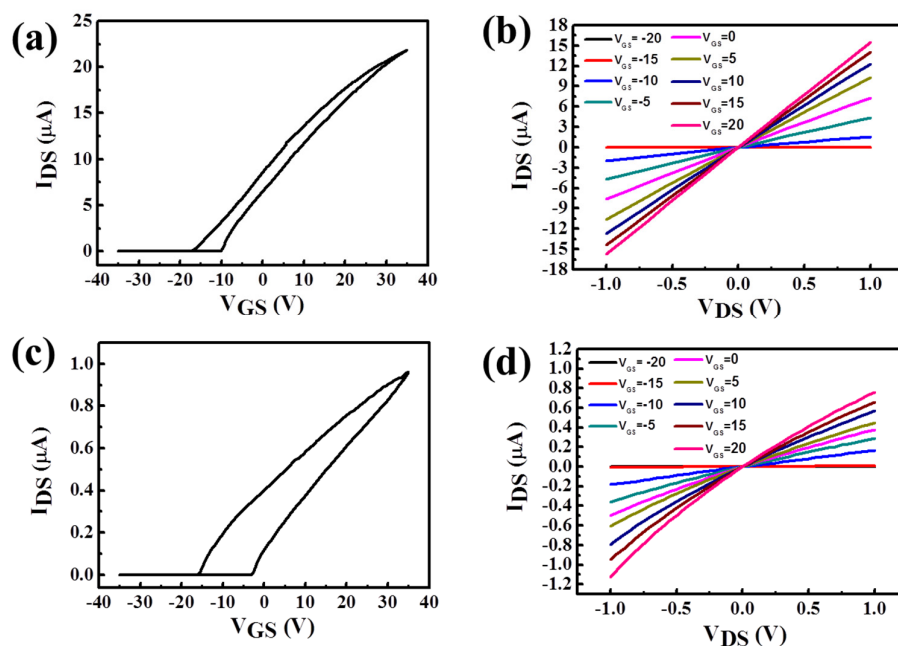


Figure S10 Electrical characterization of single NW based FETs with surface-passivation (30-nm-thick Al_2O_3) measured in ambient condition. (a) Transfer and (b) output characteristics of the In and Ga co-doped ZnO NW device. (c) Transfer and (d) output characteristics of the pristine ZnO NW device. All the source-drain bias voltage (V_{DS}) is fixed at 1 V. The scan rate is 500 mV s^{-1} .

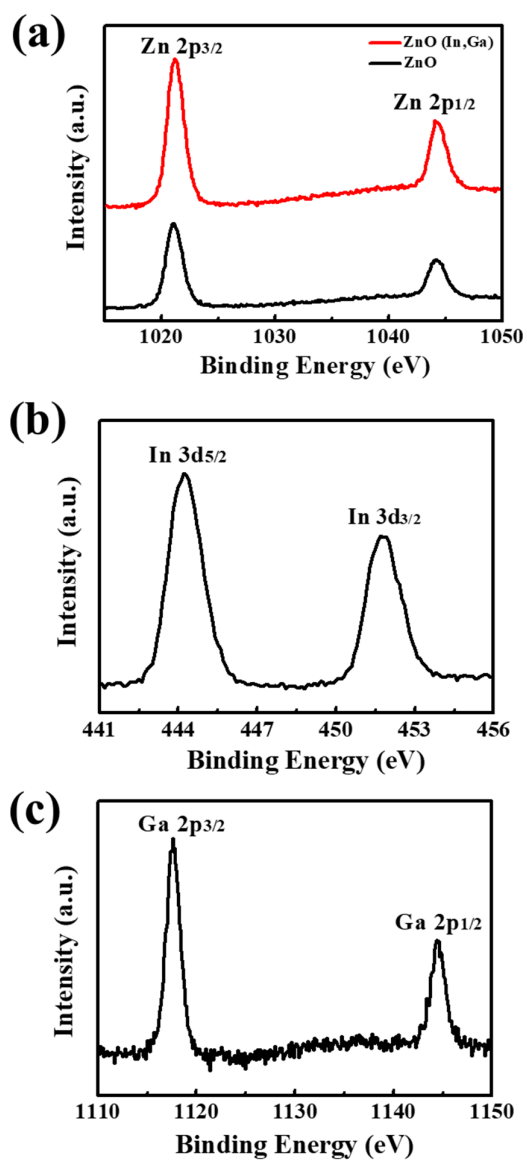


Figure S11 High-resolution XPS spectra of the (a) Zn 2p scan of both In and Ga co-doped ZnO and pristine ZnO NWs, (b) In 3d scan and (c) (d) Ga 2p scan of In and Ga co-doped ZnO NWs.

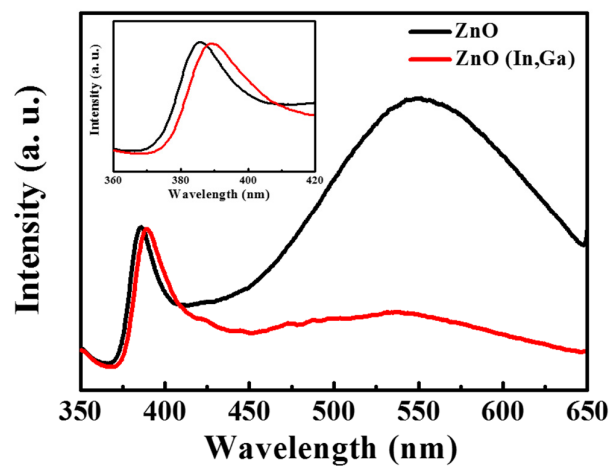


Figure S12 PL spectra of both In and Ga co-doped ZnO and pristine ZnO NWs. Inset shows the enlarged region with the range of 360 to 420 nm.

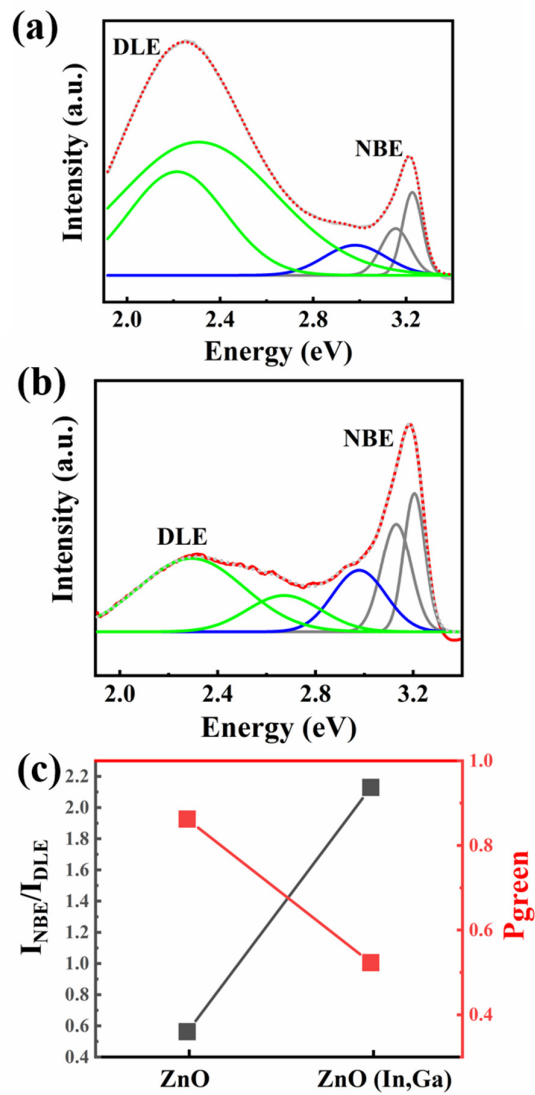


Figure S13 Deconvoluted PL spectra of (a) the pristine ZnO NWs and (b) the In and Ga co-doped ZnO NWs. (c) Variation in the peak intensity ratio of NBE/DLE and variation of green emission peak for pristine ZnO and In and Ga co-doped ZnO NW samples.

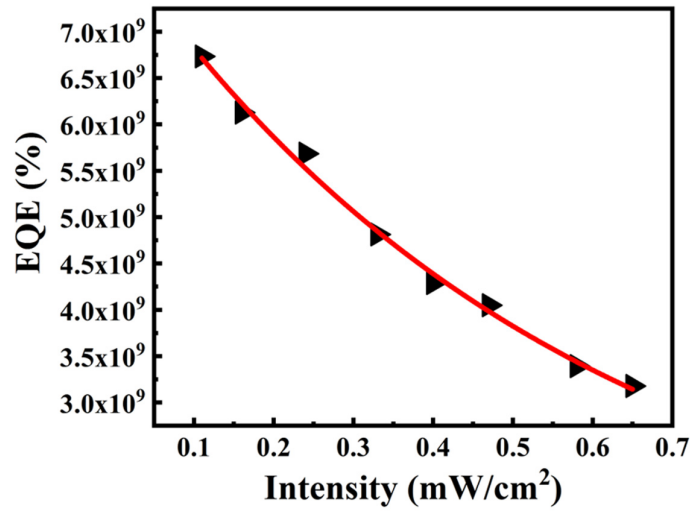


Figure S14 EQE as a function of illumination intensity for the typical In and Ga co-doped ZnO NW photodetector.

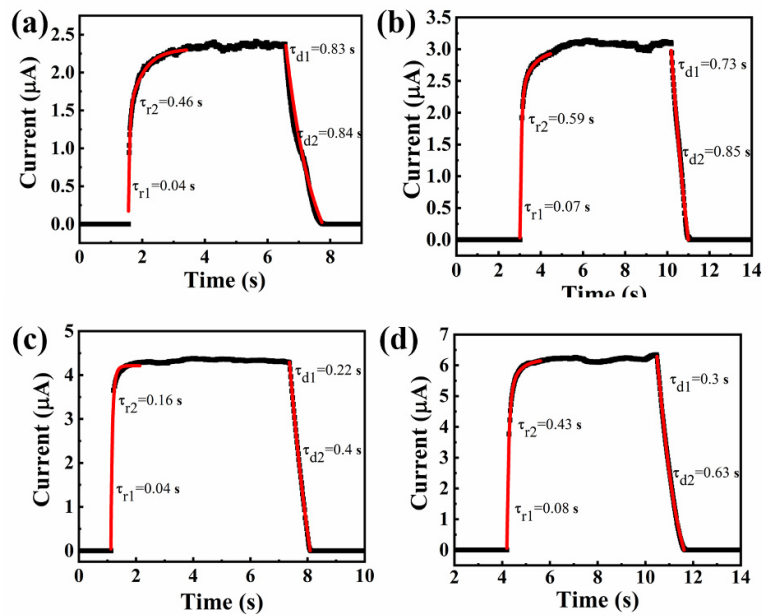


Figure S15 Photoresponse and corresponding fitting curves of In and Ga co-doped ZnO NW photodetectors under different light intensity of (a) 0.11 mW/cm² (b) 0.16 mW/cm² (c) 0.24 mW/cm² and (d) 0.65 mW/cm².

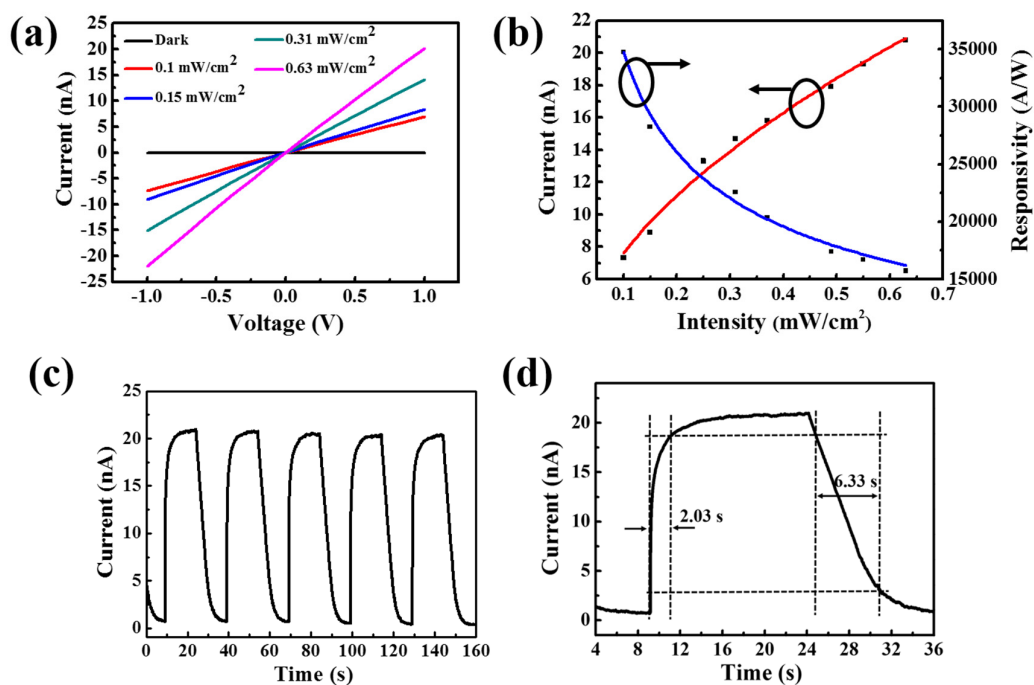


Figure S16 Current versus voltage (I-V) curve of the pristine ZnO NW photodetector measured in the dark and under different power intensity of 261 nm light illumination. Inset shows the device schematic. (b) The dependence of photocurrent and responsivity as a function of the light intensity. (c) Current versus time (I-t) and (d) high-resolution I-t curves measured under a light intensity of 0.63 mW cm⁻². $V_g = -30$ V for all panels while the applied bias is set as 1 V for panels b to d. The scan rate is 500 mV s⁻¹ for panels a and b, whereas the data collection rate is every 30 ms for panels c and d.

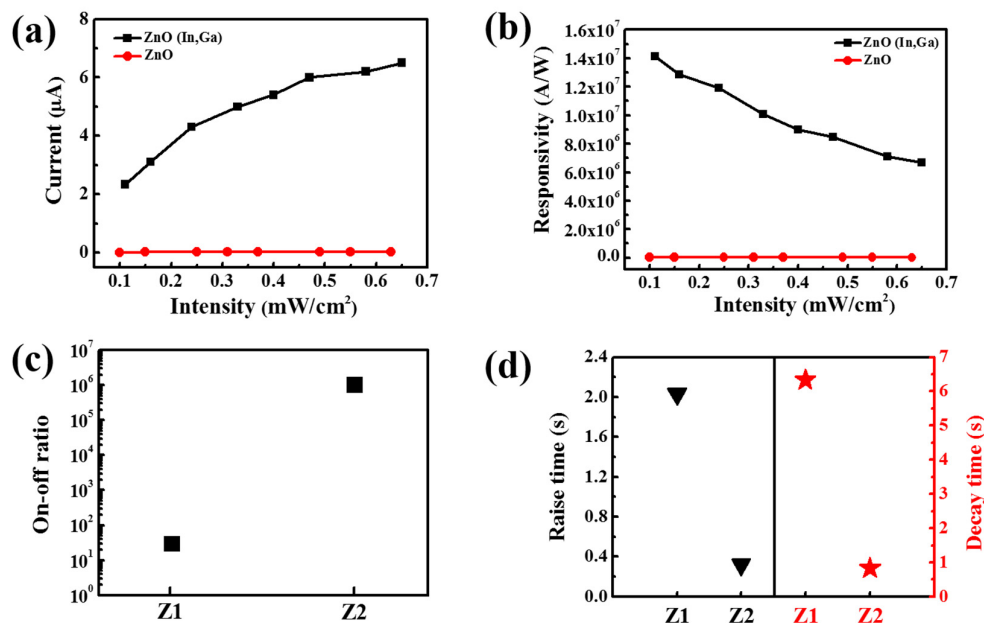


Figure S17 (a) Photocurrent versus light intensity and (b) responsivity versus light intensity of the NW photodetectors. (c) On/off ratio and (d) response time of the NW photodetectors. The bias is 1 V and $V_g = -30$ V. (Z1: pristine ZnO; Z2: In and Ga co-doped ZnO).

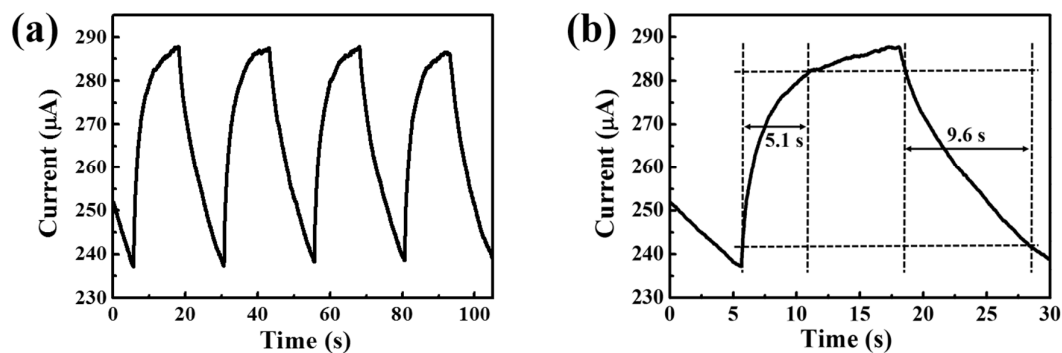


Figure S18 (a) Current versus time and (b) high-resolution current versus time curves of the In and Ga co-doped ZnO NW parallel array photodetector under a light intensity of 0.65 mW/cm^2 of 261 nm irradiation. The bias is 1 V and $V_g = -30$ V.